



¹Houshyar Eimani KALESAR, ²Eslam Doostdar SOMARIN, ³Armin ROOHBAKHSHAN

TRANSVERSE RESPONSE OF TALL BUILDINGS TAKING INTO ACCOUNT OF THE INTERFERENCE EFFECT

^{1,2} Department of Civil Engineering, Hormozgan University of Mohaghegh-Ardebil, Ardebil, IRAN

³ Department of Civil Engineering, Afarinesh Institute of Higher Education, Broujerd, IRAN

Abstract: The response of tall buildings to wind depends on many parameters, such as natural wind characteristics, surrounding environment, building size, shape, orientation, and its dynamic properties (mass, damping and stiffness). Also, location of buildings beside each other and their external shape may cause turbulent flows and complex aerodynamic problems that can significantly to the complexity of structural analysis. The analysis will become more complicated if the effect of adjacent buildings accounted in the analysis. An important effect arises when wind flows are interfered by nearly adjacent buildings. Tall buildings are not only affected in the windward direction but also are affected perpendicular to the wind direction. In many cases, the acrosswind response of tall buildings is of major concern in design. In present study, the along wind response of isolated tall rectangular buildings have been obtained for different reduced velocity by wind tunnel tests. The height of the interfering buildings was as tall as aeroelastic model. And non-dimensional acrosswind force spectrum was produced with considering neighboring effects for different reduced velocity.

Keywords: tall buildings, wind, parameters, aeroelastic model, interference effect

1. INTRODUCTION

Turbulent airflow over urban areas can significantly affect urban climate. Similarly, urban surfaces have significant influences on airflow; thus, the relation between urban surface geometry and airflow is extremely complex. Understanding this relationship is important because it affects the dispersion of air pollutants, the thermal comfort of pedestrians and heat transfer between urban surfaces and the atmosphere. Because of the complex geometries and high roughness of urban underlying surfaces, which consist of various building shapes, as well as the drag of rough surfaces in a fully developed turbulent shear flow, attenuation of airflow occurs, and the performance of natural urban ventilation is greatly influenced. It should be noted that an important characteristics of urban buildings is non-uniformity, which causes the atmo-spheric energy and mass exchange to be extremely uneven and results in unique urban climates (Arnfield, 2003; Pielke et al., 2002).

Simulating the atmospheric boundary layer (ABL) in a con-trolled environment, which makes a detailed analysis of the flow field possible, is of great importance in the fields of meteorology, civil engineering, and environmental engineering. There are currently two options for simulating ABL wind flow: boundary layer wind tunnel simulation and numerical simulation.

In the past century, development in the analysis and design of structures, advancement in construction technology and improvement in the making of light weight materials with high strength has led to the construction of tall buildings. The above mentioned parameters led to have tall buildings with high flexibility, low damping, and less weight. To take into account the above mentioned factors may cause the natural vibration frequency of structure close the frequency of vortex shedding and hence the resonance may occur. Therefore, vibration of tall buildings under wind had become a major concern for structural engineers.

Bobby et al. (2014), presents a performance-based topology optimization framework developed for wind sensitive tall buildings that rigorously accounts for the time-variant stochastic nature of the aerodynamic loads while considering additional time-invariant uncertainties describing the state/knowledge of the system parameters defining the mechanical properties of the structure.

Biao et al. (2013), investigated the wind tunnel study on the morphological parameterization of building non-uniformity. The results showed that different levels of terrain roughness have little effect on the drag coefficient. In contrast, the frontal area index is the main factor that affects the drag coefficient when the wind direction changes. The drag coefficient was found to increase with increases in the frontal area index, density index, and shape index as well as decreases in the integrated non-linear coefficient.

Tse et al. (2014), considered A comparative study of typhoon wind profiles derived from field measurements, meso-scale numerical simulations, and wind tunnel physical modeling. The comparisons focused on the simulation of the typhoon boundary layer, and revealed that a major drawback of wind tunnel testing is the use of an unrealistic approaching wind profile. As a result, the wind tunnel test results should only be considered valid when the measured wind profile is influenced predominantly by the underlying terrain.

Yi et al. (2013), presents the field measurement results of dynamic characteristics and wind-induced responses of a 420 m high tall building in Hong Kong during the passage of typhoons. The outcomes of this study are expected to be of interest and practical use to engineers and researchers who are involved in the wind-resistant design or structural health monitoring of super-tall buildings. Also Marra et al. (2011), presents a numerical algorithm for the simulation of the along-wind dynamic response of tall buildings under turbulent winds, using Monte Carlo (MC) integration methods. The results of these studies validated the appropriateness of the developed algorithm through comparison to reference values obtained from the literature for the CAARC building. Furthermore, structural "fragility curves" were utilized for a preliminary performance analysis, based on simulated along-wind response serviceability limit states.

2. PROPOSED METHODOLOGY

Figure 1 is a schematic depicting building and axis orientation, wind loading, $F_d(z, t)$, per unit height z , and bending displacements as a result of dynamic response. The dynamic displacements are denoted as $x(z, t)$ and $y(z, t)$ for the along wind and across wind dynamic response, respectively. The static response in the along-wind direction (not shown in the figure) is denoted as $\bar{X}(z)$.

The normalized mode shape of the generic mode g , which is not necessarily a linear function of the vertical coordinate z , is denoted by $\Phi_{g,d}(z)$, with the subscript $d = x$ indicating the along wind response and $d = y$ indicating the across-wind response; the mean wind incidence angle is assumed as α . The general equation of the total dynamic response in the along-wind direction, in the case that multiple structural modes are considered, can be derived by modal superposition as $x(z, t) = \sum \Phi_{g,x}(z) \xi_{g,x}(t)$, with $\xi_{g,x}(t)$ being the generalized coordinate of mode g . The main equations for the evaluation of the dynamic response for the along-wind direction in the frequency domain are summarized below:

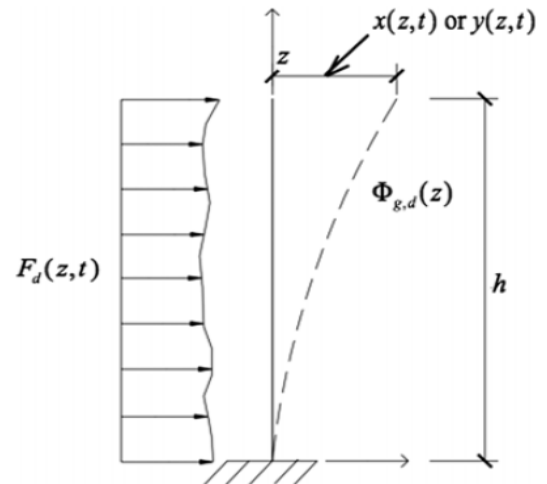


Figure 1. Schematic of building orientation, loading, and displacements

$$S_{Q_{g,x} Q_{g,x}}(n) = \rho^2 B^2 \int_0^h \int_0^h [C_D \Phi_{g,x}(z_1) \Phi_{g,x}(z_2) \bar{U}(z_1) \bar{U}(z_2) S_{uu}(n, z_1, z_2)] dz_1 dz_2 \quad (1)$$

$$= \rho^2 B^2 \int_0^h \int_0^h [\hat{f}(n, z_1, z_2)] dz_1 dz_2$$

$$S_{uu}(n, z_1, z_2) = \sqrt{S_{uu}(n, z_1) S_{uu}(n, z_2)} \exp\left(n \frac{\sqrt{C_z^2 (z_1 - z_2)^2}}{0.5 (\bar{U}(z_1) + \bar{U}(z_2))}\right) \quad (2)$$

$$S_{XX}(z, n) \cong \sum_g \frac{\Phi_{g,x}(z) \Phi_{g,x}(z) S_{Q_{g,x} Q_{g,x}}(n)}{M_{gg,x}^2 (2\pi n \eta_{g,x})^4 \left[\left(1 - \frac{n^2}{n_{0,g,x}^2}\right)^2 + \left(2 \frac{n}{n_{0,g,x}}\right)^2 (\xi_{stg,x}^* + \xi_{aerog,x})^2 \right]} \quad (3)$$

$$\sigma_X(z) = \sqrt{\int S_{XX}(z, n) dn} \quad (4)$$

Eq. (1) corresponds to the modal force spectra as a function of frequency, n , with C_D being the drag coefficient per unit vertical length, normalized with respect to the B dimension of the building (Fig. 2), measured for $\alpha = 0$. The mean wind velocity is denoted by $\bar{U}(z)$, while the height of the building by h . Eq. (2) is the cross-spectrum of the along-wind turbulence, u , at z_1 and z_2 , where $S_{uu}(n, z)$ is the longitudinal velocity spectrum. The quantity C_z is an exponential decay coefficient (Simiu et al, 1996), which is a quasisteady measure of the partial loss of coherence in the vertical direction of the pressure loading induced by turbulence (Piccardo et al, 1998). Eq. (3) describes the response auto-spectra without modal crosscoupling.

In Eq. (3), $\xi_{stg,x}^*$ is the structural damping coefficient, $\xi_{aerog,x}$ is the aerodynamic damping (Simiu et al, 1996), and $M_{gg,x}$ is the modal mass. Eq. (4) describes the root mean square (RMS) response, derived from Eq. (3).

The previous equations assume that the response in the x -direction and the y -direction is dominated by the two fundamental and mutually orthogonal bending modes ($g = 1$) with mode shapes $\Phi_{1,x}(z)$ and $\Phi_{1,y}(z)$. Structural and aerodynamic coupling was

neglected at this time between the x-direction and the y-direction components. Even though the results will not be presented in this paper, additional simulations were conducted to determine the potential influence of modal aerodynamic coupling between the two primary bending planes (Simiu et al, 1996. Caracoglia, 2007). Effects of uncertainty in the characterization of aerodynamic loading and their influence on the dynamic response were simulated through MC algorithms. In this study uncertainty associated with modeling and experimental errors was simulated by appropriate random perturbation applied to some of the parameters in Eqs. (1)–(4), such as C_z or C_D , about a reference deterministic value. The proposed methodology utilizes MC methods to accomplish the following steps: (1) compute the power spectral density of the modal buffeting force (Eq. (1)) as a function of frequency, restricted to $g = 1$ in the following examples, by numerical integration; and (2) derive statistical information about the dynamic response when uncertainty in the characterization of dynamic loading is accounted for. By combining Steps 1 and 2, a “Two-Step Monte Carlo Algorithm” was developed and implemented to estimate the along-wind dynamic response of a high-rise building. The two-step MC procedure enabled the numerical calculation of a generic surface integral, $\hat{f}(n, z_1, z_2)$, being the function enclosed within brackets in Eq. (1) and corresponding to the modal spectral loading. This surface integral was evaluated by utilizing a set of randomly generated and uniformly distributed numbers (integration points) to numerically estimate the statistical expectation of the function $\hat{f}(n, z_1, z_2)$ (Robert et al, 2004). In the case of the double integral, there are two randomly generated samples of size NMC defined on the intervals $[Z_0, Z_A]$ and $[Z_0, Z_B]$, where the variables $Z_0 = 0$, $Z_A = h$ and $Z_B = h$ are the integration limits along the height of the structure. The following equation gives the general form of the equation used to approximate the double integral in Eq. (1) with integrand $\hat{f}(n, z_1, z_2)$:

$$\int_{Z_0}^{Z_A} \int_{Z_0}^{Z_B} [\hat{f}(n, z_1, z_2)] dz_1 dz_2 \cong E [\hat{f}(n, z_1, z_2)] (Z_A - Z_0) (Z_B - Z_0). \quad (5)$$

The previous equation would be exact if the estimation of the expectation $E[\hat{f}(n, z_1, z_2)]$ were based on an infinite sample.

Since the assessment of $E[\hat{f}(n, z_1, z_2)]$ relies on arithmetic averaging (practically), the right hand side of the integral is approximate (Robert et al, 2004). Therefore, the inequality sign was employed in Eq. (5) because the assessment of expectation is inexact.

3. WIND TUNNEL CONDITIONS FOR RESEARCHES IN THIS STUDY

To obtain spectrum of nondimensional force, considering the interference effect of high buildings, wind tunnel simulation criteria have been carried out as follows: The length of tunnel is 38.5 meters. The width and height of the tunnel is about 2 x 2 meters. The maximum height of the boundary layer The maximum height of the boundary layer, can be created without using additional instruments and smooth floor is about 20 cm.

4. SIMULATION OF WIND SPEED PROFILES IN WIND TUNNEL

Profiles of wind speed in the tunnel is shown in Figure 2, that with the wind velocity profile in nature, and environmental conditions ($\alpha = 0.3$) compared. For the experiments in this study, two types of models have been used:

1. aeroelastic model,
2. rigid models.

That aeroelastic model is for modeling behavior of the main building and rigid models are for modeling behavior of adjacent building.

4.1. Transverse response of tall buildings taking into account of the interference effects

In this study, two modes for arrangement of the main building and adjacent structures have been studied:

1. The main building, as Short Afterbody (SAB), namely large dimension perpendicular to the wind direction. And adjacent buildings as Long Afterbody (LAB), namely small dimension perpendicular to the wind direction.
2. Both of the main and adjacent building are as SAB.

To obtain spectrum of nondimensional force, initially the adjacent building is placed at different distances from the main building. Figure 3 shows a schematic arrangement of the main building in the state sab, and adjacent buildings in the state LAB. In this study, for record the displacement at the top of structure in each experiment, at least 4000 samples are tested.

4.2. Obtain the Nondimensional transverse force spectra for aeroelastic model with interference of M_1 and M_2 model

In this section, spectrum of Nondimensional transverse force when the aeroelastic model is in SAB mode and rigid model is in LAB mode, Has been investigated. For a constant reduced velocity, by changing the position of the M_1 and M_2 model, wind flow patterns have changed on the aeroelastic model. Consequently, the structural response and Spectrum of transverse force is

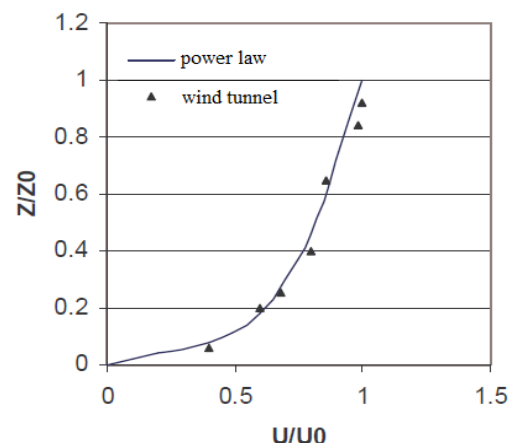


Figure 2. Comparison of average velocity profiles in the altitude wind tunnel with power law relationship ($\alpha = 0.3$)

changed. Nondimensional transverse force spectra for aeroelastic model with interference of M_1 and M_2 model for reduced velocity 5.9, 8.14, 10.21 and 12.5 are shown in Figures 4 to 7. For investigate the changes in Spectrum of Nondimensional transverse force, the maximum Spectrum of transverse force for different reduced velocity is presented in Table 1.

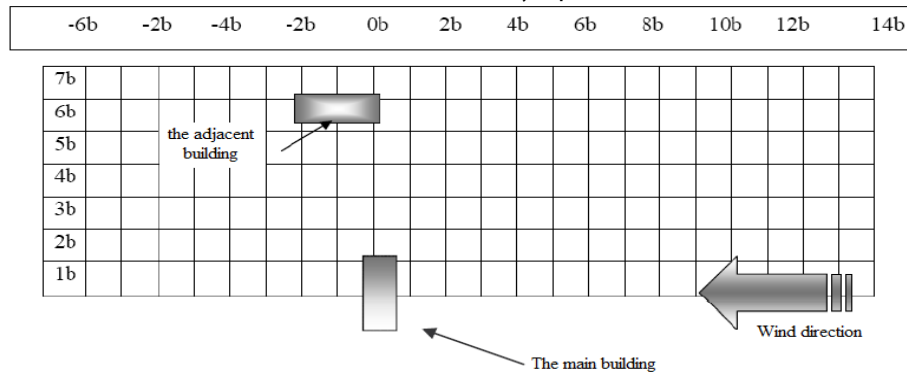


Figure 3. Arrangement of the main building in the state SAB, and adjacent buildings in the state LAB.

Table 1. The change process of maximum Spectrum of the transverse force

reduced velocity (R_v)	M_1 model			M_2 model		
	Position of model X	Y	The maximum Spectrum of transverse force	Position of model X	Y	the maximum Spectrum of transverse force
5.90	10B	2.5B	0.014	8B	0.5B	0.107
8.14	12B	0B	0.432	8B	0.5B	0.235
10.21	5B	0B	0.596	8B	0.5B	0.420
12.50	12B	0B	1.579	9B	0B	8.144
14.48	14B	3.5B	56.136	16B	1.5B	73.673
15.71	10B	1.5B	28.47	4B	1.5B	42.508
16.51	14B	1.5B	7.944	8B	2.5B	10.345

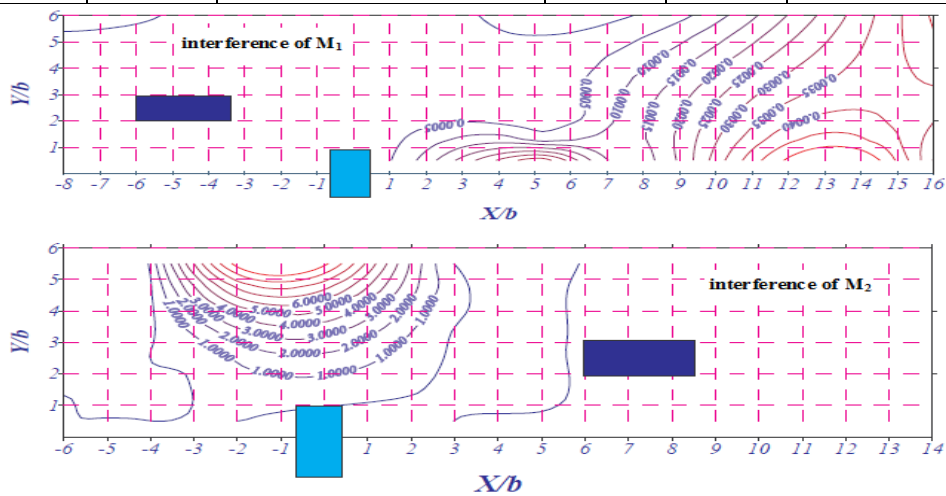


Figure 4. Spectrum of Nondimensional transverse force for $R_v=5.9$

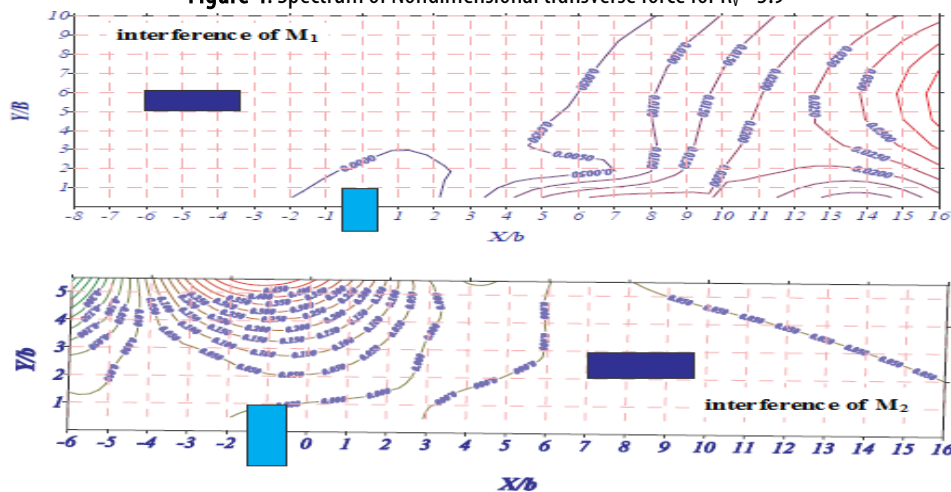


Figure 5. Spectrum of Nondimensional transverse force for $R_v=8.14$

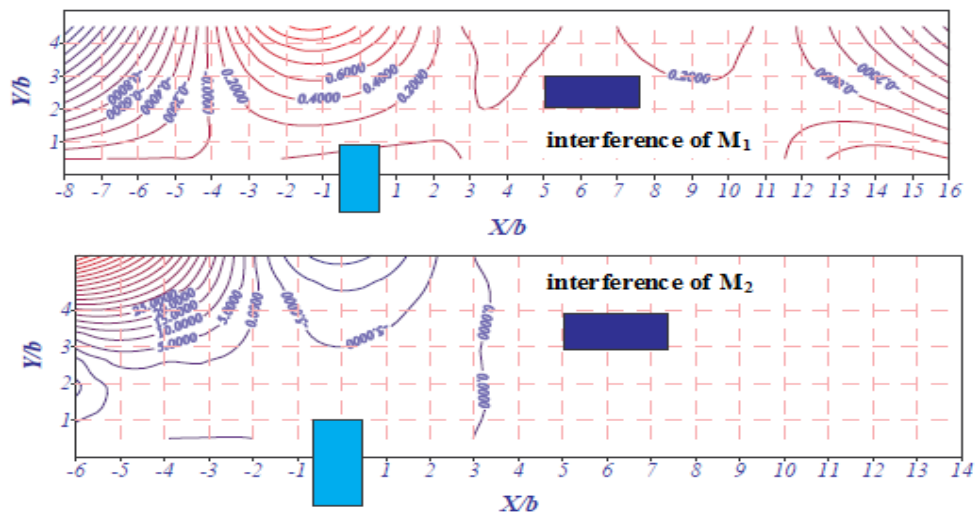


Figure 6. Spectrum of Nondimensional transverse force for $R_v=10.21$

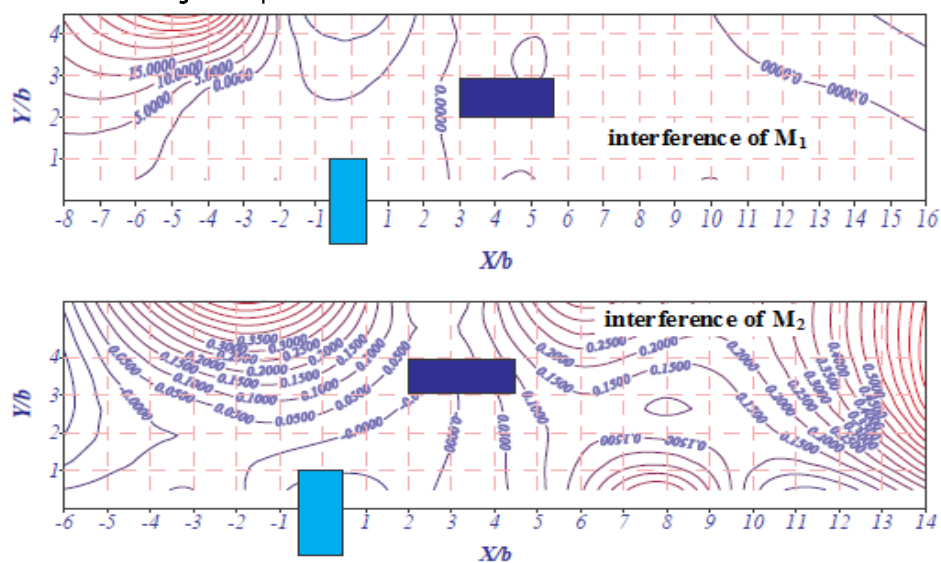


Figure 7. Spectrum of Nondimensional transverse force for $R_v=12.5$

5. CONCLUSIONS

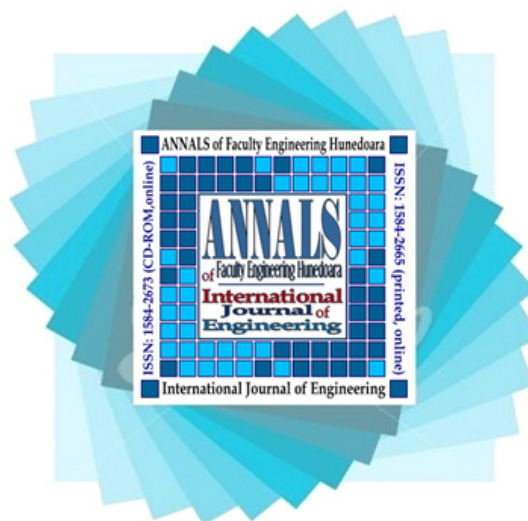
In present study, the along wind response of isolated tall rectangular buildings have been obtained for different reduced velocity by wind tunnel tests. Therefore, some conclusions from this study are summarized as follows:

- » Considering the interference effect of high buildings, determined that the amount of transverse force spectrum, along the perpendicular to the wind, in the tall rectangular building, depends on the average speed of wind, arrangement and the position of adjacent building.
- » The comparisons show that, by increasing the length of the adjacent buildings, spectrum of Non-dimensional transverse force increased.
- » Engineers in the design of tall buildings, consider the interaction in the calculations.

References

- [1.] Arnfield, A.J. Two decades of urban climate research: a review of turbulence, exchanges of energy and water, and the urban heat island urban climate; urban energy budget; urban water budget; urban heat island; urban atmospheric turbulence; urban roughness; spatial heterogeneity. *International Journal of Climatology: a Journal of the Royal Meteorological Society* 23 (1), 1–26. 2003.
- [2.] B, Li . J, Liu, M, Li. Wind tunnel study on the morphological parameterization of building non-uniformity. *J. Wind Eng. Ind. Aerodyn.* 121: 60–69. 2013.
- [3.] Bobby, S. Seymour M.J. Spence. Bernardini, E. Kareem,A. Performance-based topology optimization for wind-excited tall buildings: A framework. *Engineering Structures* 74 (2014) 242–255. 2014.
- [4.] Caracoglia L. Influence of weather conditions and eccentric aerodynamic loading on large amplitude aeroelastic vibration of highway tubular poles. *Eng Struct*; 29: 3550–66. 2007.

- [5.] J. Yi, J.W. Zhang, Q.S. Li. Dynamic characteristics and wind-induced responses of a super-tall building during typhoons. *J. Wind Eng. Ind. Aerodyn.* 121 : 116–130. 2013.
- [6.] K.T. Tse, S.W. Li , J.C.H. Fung. A comparative study of typhoon wind profiles derived from field measurements, meso-scale numerical simulations, and wind tunnel physical modeling. *J. Wind Eng. Ind. Aerodyn.* 131 : 46–58. 2014.
- [7.] M.A. Smith, L. Caracoglia. A Monte Carlo based method for the dynamic “fragility analysis” of tall buildings under turbulent wind loading. *Engineering Structures* 33 : 410–420. 2011.
- [8.] Piccardo G, Solari G. Generalized equivalent spectrum technique. *Wind Struct*;1(2):161–74. 1998.
- [9.] Pielke, R.A., Marland, G., Betts, R.A., et al. The Influence of land-use change and landscape dynamics on the climate system: relevance to climate-change policy beyond the radiative effect of greenhouse gases. *Philosophical Transactions Series A, Mathematical, Physical, and Engineering Sciences* 360 (1797), 1705–1719. 2002.
- [10.] Robert CP, Casella G. Monte Carlo statistical methods. New York: Springer Science; 2004.
- [11.] Simiu E, Scanlan RH. Wind effects on structures. New York: John Wiley & Sons, Inc; 1996.



ANNALS of Faculty Engineering Hunedoara – International Journal of Engineering



copyright © UNIVERSITY POLITEHNICA TIMISOARA, FACULTY OF ENGINEERING HUNEDOARA,
5, REVOLUTIEI, 331128, HUNEDOARA, ROMANIA
<http://annals.fih.upt.ro>